Chemosphere 158 (2016) 143–153

Contents lists available at ScienceDirect

Chemosphere

journal homepage: www.elsevier.com/locate/chemosphere

Perfluorooctanoic acid exposure alters polyunsaturated fatty acid composition, induces oxidative stress and activates the AKT/AMPK pathway in mouse epididymis

Yin Lu [a], Yitao Pan [a], Nan Sheng [a], Allan Z. Zhao [b, **], Jiayin Dai [a, *]

[a] Key Laboratory of Animal Ecology and Conservation Biology, Institute of Zoology, Chinese Academy of Sciences, Beijing, 100101, China
[b] Center of Metabolic Disease Research, Nanjing Medical University, Nanjing, 210029, China

HIGHLIGHTS

- PFOA exposure altered polyunsaturated fatty acid composition in epididymides.
- Triglyceride level and AKT/AMPK signaling strength were detected.
- PFOA exposure resulted in oxidative stress in the epididymis.

ARTICLE INFO

Article history:
Received 25 February 2016
Received in revised form
2 May 2016
Accepted 22 May 2016
Available online 1 June 2016

Handling Editor: A. Gies

Keywords:
PUFA
Oxidative stress
ROS

ABSTRACT

Perfluorooctanoic acid (PFOA) is a degradation-resistant compound with a carbon-fluorine bond. Although PFOA emissions have been reduced since 2000, it remains persistent in the environment. Several studies on laboratory animals indicate that PFOA exposure can impact male fertility. Here, adult male mice received either PFOA (1.25, 5 or 20 mg/kg/d) or an equal volume of water for 28 d consecutively. PFOA accumulated in the epididymis in a dose-dependent manner and resulted in reduced epididymis weight, lower levels of triglycerides (TG), cholesterol (CHO), and free fatty acids (FFA), and activated AKT/AMPK signaling in the epididymis. Altered polyunsaturated fatty acid (PUFA) compositions, such as a higher arachidonic acid:linoleic acid (AA:LA) ratio, concomitant with excessive oxidative stress, as demonstrated by increased malonaldehyde (MDA) and decreased glutathione peroxidase (GSH-Px) in the epididymis, were observed in epididymis tissue following treatment with PFOA. These results indicate that the epididymis is a potential target of PFOA. Oxidative stress and PUFA alteration might help explain the sperm injury and male reproductive dysfunction induced by PFOA exposure.

1. Introduction

Perfluoroalkyl substances (PFASs) are manmade compounds with strong carbon-fluorine bonds of varying length. PFASs are widely used in industrial products and have become widespread in environmental matrices (Pico et al., 2011). Among all PFASs, eight-carbon-chain perfluorooctanoic acid (PFOA) and perfluorooctanesulfonate (PFOS) are among the most widely detected and studied. Although they have both been phased out or restricted in some countries since 2000 (Dimitrov et al., 2004; Lehmler, 2005), PFOA is still persistent in the environment due to its continual production in some areas lacking legal restrictions as well as via the degradation of its precursors (Prevedouros et al., 2006; Wang et al., 2009). In addition, PFOA can be accumulated in the blood, liver and testes in a dose-dependent manner. For example, 28 d of exposure to 1.25–20 mg/kg/d PFOA via oral gavage was found to increase PFOA residue in the blood (20–110 μg/mL), liver (80–140 μg/g), and testes (1–9 μg/g) of laboratory mice (Yan et al., 2014, 2015; Zhang et al., 2014a).

As a fatty acid analogue, PFOA exposure may be associated with increased cholesterol (CHO) and triglyceride (TG) levels in human blood (Steenland et al., 2009). Tight regulation between TG synthesis, hydrolysis, secretion and fatty acid oxidation is required to prevent lipid accumulation and/or depletion from cells (Mantzaris et al., 2011). Activation of AMP-activated protein kinase (AMPK) and

* Corresponding author.
** Corresponding author.
E-mail address: daijy@ioz.ac.cn (J. Dai).

http://dx.doi.org/10.1016/j.chemosphere.2016.05.071
0045-6535/

AKT (also known as protein kinase B, PKB) regulates lipid metabolism by stimulating fatty acid uptake and promoting energy use by increasing total cellular ATP content via glycolysis and oxidative phosphorylation control (Bellacosa et al., 1991; Lan and Du, 2015). In addition, AMPK stimulation has been reported to restore lipid metabolism disorder in ob/ob mice (Samovski et al., 2015; Zeng et al., 2015).

Fatty acids are precursor molecules for the synthesis of lipids, which influence membrane fluidity, lipid raft structures, and signal transduction (Papackova and Cahova, 2015). Omega-3 and omega-6 polyunsaturated fatty acids (PUFA) are two fatty acid families necessary in vertebrates and obtained through hydrolysis of TG from food (Funari et al., 2003; Thomas et al., 2004). Among them, arachidonic acid (AA) and ω-6 PUFA promote oxidative reactions in the presence of iron and use iron as an oxidative stress inducer both *in vivo* and *in vitro* (Shin et al., 2009; Dong et al., 2013). Under oxidative conditions, excessive reactive oxygen species (ROS) are released, which alter the sperm membrane structure (Shin and Kim, 2009), and can lead to diseases such as cancer, autoimmune disorders, and liver, cardiovascular and neurodegenerative diseases (Auten and Davis, 2009).

The aim of the present study was to gain insight into the effects of PFOA on TG content and PUFA composition, as well as explore oxidative stress parameters and the AKT/AMPK signaling pathway, in the epididymis of mice, and thus provide rationale for the potential toxicity induced by PFOA.

2. Material and methods

2.1. Animals and PFOA treatment

Eighty BABL/c male mice (6–8 weeks old, 20–27 g) were housed in a temperature (23 ± 1 °C) and humidity (60 ± 5%) controlled room under a constant 12/12 h light/dark cycle. All procedures were performed in accordance with protocols approved by the Ethics Committee of the Institute of Zoology, Chinese Academy of Sciences. Mice were randomly divided into four groups of equal size. The mice received either PFOA by oral gavage at doses of 1.25, 5, or 20 mg/kg/d, or an equal volume of sterile Milli-Q water for the control group. The PFOA doses were selected based on earlier research (Yan et al., 2014). After 28 d of exposure, all mice were weighed, and the epididymides were dissected for immediate use or kept at −80 °C until further analysis.

2.2. Epididymis PFOA measurement

The PFOA concentrations in mice epididymides were measured using an ion-pair liquid-liquid extraction method (Hansen et al., 2001). In brief, a homogenate of 50 mg of epididymis to 1 mL of water was prepared. The homogenate was spiked with 0.4 ng of mass-labeled standard, 1 mL of tetra-*n*-butylammonium hydrogen sulfate solution (TBAS, 0.5 M), 2 mL of $NaHCO_3/Na_2CO_3$ buffer solution (pH = 10), and 4 mL of methyl *tert*-butyl ether (MTBE). The mixture was shaken at 250 rpm for 20 min at room temperature and centrifuged at 4000 rpm for 15 min until layers were well separated. The organic supernatant was transferred to a new tube. The extraction procedure was repeated twice. All three extracts were combined and evaporated to dryness under a gentle stream of nitrogen gas at 40 °C and reconstituted with 200 μL of methanol.

Samples were analyzed by an Acquity UPLC coupled to a Xevo TQ-S triple quadrupole mass spectrometer (Waters, Milford, MA, USA) in negative electrospray ionization (ESI-) mode. Chromatographic separation was accomplished using an Acquity BEH C18 column (100 mm × 2.1 mm, 1.7 μm, Waters, MA, USA) with mobile phases: 10 mM ammonium acetate in water (A) and methanol (B) at a flow rate of 0.4 mL/min. Target compounds were determined by multiple reaction monitoring (MRM) in negative ionization (ESI-) mode. The MRM transitions were 413 → 369 for PFOA (cone voltage, 20 V; collision energy, 10 V) and 417 → 372 for $^{13}C_4$-PFOA (cone voltage, 20 V; collision energy, 9 V).

Calibration curves (range: 0.05–20 ng/mL) exhibited excellent linearity ($R^2 > 0.999$). Matrix recovery of PFOA was 93% (n = 5). The limit of quantitation (LOQ) was defined as the lowest standard having a signal-to-noise ratio greater than 10, and was 0.05 ng/mL for PFOA. In each batch, two method blanks and two matrix spiked samples were run for quality assurance. No detectable contamination was found in any batch.

2.3. Histological analysis

Epididymides from the control mice and the 1.25, 5, and 20 mg/kg/d PFOA-exposed mice were fixed in 4% paraformaldehyde and embedded in OCT compound (Sakura Finetek USA, Torrance, CA, USA). Frozen sections (5 μm) were prepared and then processed for hematoxylin and eosin (H&E) staining.

2.4. Polyunsaturated fatty acid extraction and gas chromatography

Frozen epididymides from the control and 5 mg/kg/d PFOA-treated mice were thawed and prepared for PUFA composition detection using gas chromatography (GC). Approximately 25 mg of epididymis was homogenized in 1.5 mL of Milli-Q water using a tissue disintegrator and ultrasonic cell disruptor. The homogenized tissue was mixed with 6 mL of extract solvent (methanol/chloroform, 2:1, v:v) and internal standard (50 μg, C19:0, Sigma-Aldrich, St Louis, MO, USA), then vortex oscillated for 10 s, and kept at room temperature for 15 min. Chloroform and water (2 mL, respectively) were added and the suspension was vortex oscillated for 10 s, incubated at room temperature for 1 min, then centrifuged at 1500*g* for 30 min at 16 °C. The lowest layer was obtained by centrifugation of the suspension at 1500*g* for 30 min at 16 °C, before being transferred to a new glass tube, and dried under a gentle stream of nitrogen gas at 35 °C. The residue was reconstituted in 1.5 mL of boron trifluoride/methanol (14%), caped and vortex oscillated, then incubated at 90 °C for 30 min. After cooling for 10 min, 4.0 mL of pentane and 1.5 mL of water were added to the *trans*-methylated fatty acids, which was then caped, vortex oscillated, and centrifuged at 1500*g* for 2 min at room temperature. The supernatant was transferred to a new glass tube and dried under a gentle stream of nitrogen gas at 35 °C. The residue was reconstituted and extracted with 400 μL of hexane and 100 μL of heptane and vortex oscillated for 10 s, with 2.0 μL then injected for GC analysis.

An Agilent GC 7890 gas chromatograph (Agilent, Waldbronn, Germany) was utilized throughout the experiments and a GC capillary column (SP-2380 105 m × 0.53 mm × 0.20 μm, Supelco, USA) was used. Separation was performed with the following temperature gradient: constant 140 °C with 8 °C/min for 35 min and constant 220 °C for 12 min. The sample injector was operated at 260 °C, and the carrier gas for both sections was helium (purity 99.9999%) with a flow pressure at 15 psi and speed at 28 mL/min. The flame ionization detector was operated at 260 °C, with helium flow pressure at 12 psi and speed at 5 mL/min. Under these conditions, all biologically relevant PUFAs were baseline separated, as shown by a PUFA standard (PUFA No.2, 47015, Sigma-Aldrich, St Louis, MO, USA). Agilent ChemStation Rev B.03.01 was used for instrument control and data handling. Components were identified by comparing retention time with authentic standards. Quantification of PUFA was carried out based on their peak areas compared with the internal standard (C19:0) peak area, and the percentages

of each PUFA were calculated.

2.5. Measurement of triglycerides, cholesterol and free fatty acids in the epididymis

Epididymides were dissected from mice that received PFOA at doses of 1.25, 5, or 20 mg/kg/d, or an equal volume of water. The epididymis was placed in 10% physiological saline or lysis buffer and homogenized. The supernatant was obtained by centrifugation of the homogenates at 4000*g* for 10 min. The following detections were performed using commercial kits according to the manufacturer's instructions (TG and CHO, Applygen Technologies, Beijing, China; free fatty acids (FFA), Nanjing Jiancheng Bioengineering Institute, Nanjing, China). All final data were normalized to the epididymis protein concentration detected by the bicinchoninic acid method (Tiangen Biotech Corporation, Beijing, China).

2.6. Sperm preparation and ROS detection

Currently, no method for measuring ROS in the epididymis exists, accordingly, we investigated sperm *in vitro* to clarify the effect of PFOA on ROS content. The procedure for retrieving sperm was as follows: cauda epididymides were dissected from adult BABL/c male mice (10–12 weeks) and washed with phosphate buffer solution (PBS). Cauda epididymides were punctured by syringe and then placed in phenol red-free M199 medium (Cat. 11043; Thermo Fisher Scientific Inc., Waltham, MA, USA) to allow for the release of sperm at 37 °C and 5% CO_2. After 20 min, sperm in the suspension were washed in M199 medium followed by centrifugation at 800*g* for 10 min. Sperm were then resuspended to a final concentration of 2×10^6 cells per ml and diluted in M199 medium. The sperm were incubated in 1:1000 diluted DCFH-DA medium (Beyotime Institute of Biotechnology, Hangzhou, China) at 37 °C to load the probe. After 20 min, the sperm were washed in M199 medium and exposed to PFOA at doses of 0, 100, and 400 μM or 1:1000 Rosup diluted in M199 medium as a positive control. At the exposure times of 1 h, 2 h, 4 h, and 8 h, ROS analysis was performed to measure 2′,7′-dichlorofluorescein (DCF) in cells using a fluorescence microplate reader. Sperm ROS levels were normalized to sperm viability using a CCK-8 kit (Solarbio Technology Co., Ltd., Beijing, China).

2.7. Detection of SOD, MDA, and GSH-Px

Epididymides were dissected from mice exposed to PFOA at doses of 1.25, 5, or 20 mg/kg/d, or an equal volume of water. The epididymides were placed in 10% physiological saline and homogenized. The supernatant was obtained by centrifugation of the homogenates at 4000*g* for 10 min. The protein concentration of the supernatant was measured using the BCA method. The detections of superoxide dismutase (SOD), malonaldehyde (MDA), and glutathione peroxidase (GSH-Px) were performed via the nitroblue tetrazolium-illumination method, thiobarbituric acid method, and benzoic acid method, respectively (Loh et al., 2010; Liu et al., 2013; Zhang et al., 2014b) using commercially available kits (Nanjing Jiancheng Bioengineering Institute, Nanjing, China).

2.8. RT-PCR analysis

RT-PCR analysis was performed to detect mRNA levels. Epididymides from the control and PFOA-treated (1.25, 5, and 20 mg/kg/d) groups were randomly selected. Total RNA was extracted by Trizol reagent, and was performed as described previously (Zhang et al., 2014a). The presence of mRNA transcripts within the epididymis was normalized to the mean level of the internal control gene 18S. The authenticity of the mRNA transcripts detected in the epididymis was confirmed by nucleotide sequencing. Mouse-specific primers are listed in Table S1.

2.9. Western blot analysis

Preparation of the protein extracts from the testes and epididymides and western blot analyses were performed as described previously (Feng et al., 2009, 2010). Protein extracts were prepared with RIPA buffer supplemented with protease inhibitor (PMSF) and protein phosphatase inhibitors (Applygen Technologies, Beijing, China). P-AMPK (Thr172), AMPK, p-AKT (Thr308), p-AKT (Ser473), and AKT primary antibodies were purchased from Cell Signaling Technology (Danvers, MA, USA), and diluted to 1:1000. APOA1 primary antibody was purchased from Abcam (Cambridge, MA, UK), and diluted to 1:5000. The protein bands were visualized by enhanced chemiluminescence (superECL, Tiangen, Beijing, China) on X-ray films and analyzed with Quantity One software (v 4.6.3, Bio-Rad, USA). Data were normalized to protein expression levels of β-actin or GAPDH and the control data were set as 1. All results were presented as mean ± SE for each group of at least three individual samples.

2.10. Statistical analysis

Comparison between groups was performed using one-way analysis of variance (ANOVA), followed by Tukey's honestly significant difference test and Duncan's multiple range test, or the independent-samples *t*-test using SPSS software (Version 18, SPSS, Inc., Chicago, IL, USA). All data were presented as mean ± SE. Probability levels of $P < 0.05$ were considered significant.

3. Results

3.1. PFOA exposure increased epididymis damage

Male mice that received either PFOA (1.25, 5, or 20 mg/kg/d) or an equal volume of water were analyzed. After sacrifice, the epididymis and mouse body weights were obtained. The relative epididymis weight was calculated by dividing the epididymis weight by body weight. Epididymis weight was reduced in mice treated with 5 or 20 mg/kg/d PFOA (Fig. 1A), and the relative epididymis weight was also reduced in mice treated with 20 mg/kg/d PFOA, but unchanged in mice treated with 5 mg/kg/d PFOA (Fig. 1B). Moreover, PFOA accumulated in the epididymis of male mice in a dose-dependent manner (Fig. 1C). Morphologically, the structure of caput, corpus and cauda epididymis from the control group was integrated, seminiferous ducts and muscle fibers around them were well-organized, and the tubulars of cauda were full of sperms. The 1.25 mg/kg/d PFOA group shown no visible morphological changes, while the cauda epididymis from 5 to 20 mg/kg/d PFOA groups were observed small empty spaces in tubulars, illustrated lacking of normal sperm in mice cauda epididymis treated with 5 and 20 mg/kg/d PFOA, when epididymis sections were analyzed (Fig. 1D).

3.2. PFOA exposure diminished lipid levels in the epididymis

Epididymal levels of TG and CHO were measured in male mice receiving either PFOA (1.25, 5, or 20 mg/kg/d) or an equal volume of water. In addition, the levels of FFA in the control and 5 mg/kg/d PFOA-treated mice were measured. Epididymal TG content was significantly decreased in the 5 and 20 mg/kg/d PFOA exposure groups (Fig. 2A). A reduction in epididymal CHO and FFA in the 20 and 5 mg/kg/d PFOA exposure groups, respectively, was also

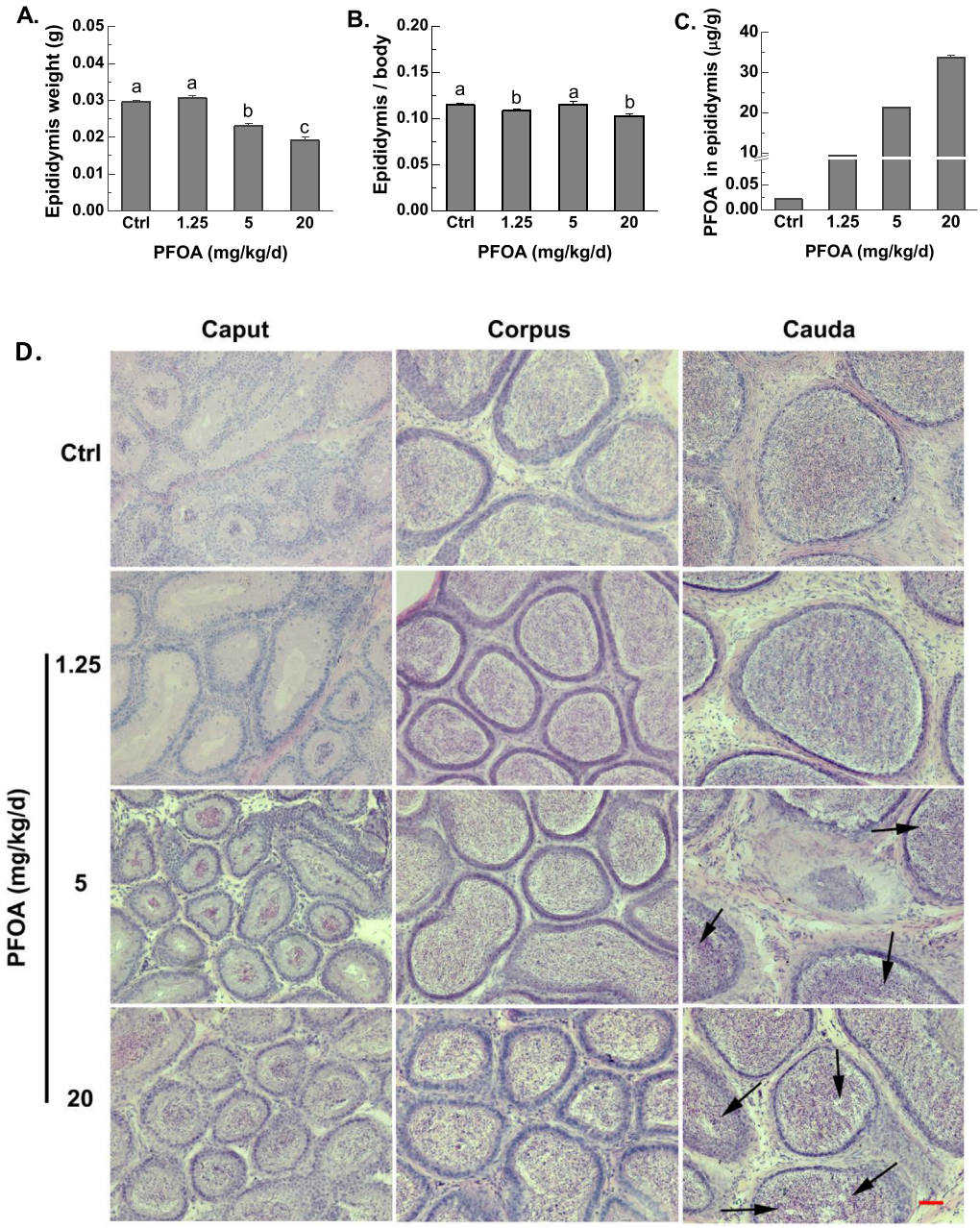

Fig. 1. PFOA exposure caused epididymis damage in mice. (A) Epididymis weight (n = 11). (B) Relative epididymis weight (n = 11). Mice received either PFOA at 1.25, 5, or 20 mg/kg/d or an equal volume of water for 28 d consecutively. Whole mice and their epididymides were weighed, relative weights were calculated by dividing epididymis weight by body weight. All data are means ± SE. Values not sharing a common superscript differ significantly at $p < 0.05$ by ANOVA and Duncan's multiple range tests. (C) PFOA levels in the epididymis (n = 3). (D) Representative images of hematoxylin and eosin (H&E) stained epididymis cross-sections from the control and PFOA-exposed groups (scale bar is 50 μm).

observed (Fig. 2A and Fig. S1). As for the genes related to TG, CHO, and FFA metabolism processes, the levels of monoglyceride lipase (MGL) in the 5 and 20 mg/kg/d PFOA exposure groups and Niemann-Pick disease, type C1 (NPC1) mRNA were decreased in the 20 mg/kg/d PFOA exposure groups, and HMG-CoA reductase (HMG-COA R) gene expression was decreased in the 5 and 20 mg/kg/d PFOA exposure group (Fig. 2C). Apolipoprotein A-I (APOA1) protein levels were also reduced in the 1.25 and 5 mg/kg/d PFOA exposure groups, but were increased in the 20 mg/kg/d PFOA exposure group (Fig. 2D). The expressions of other genes, including adipose triglyceride lipase (ATGL), hormone-sensitive lipase (HSL), Niemann-Pick disease, type C2 (NPC2), high density lipoprotein binding protein (HDLBP), scavenger receptor class B, member 1 (SRB1), and low-density lipoprotein receptor (LDLR), were not significantly altered (Fig. S1).

3.3. PFOA altered polyunsaturated fatty acid composition in the epididymis

Mice epididymides were obtained from the control and 5 mg/kg/d PFOA-treated mice. Following FFA extraction, PUFA composition was analyzed using gas chromatography. Generally, the levels of PUFAs containing less than 18 carbon atoms decreased, whereas PUFAs containing more than 20 carbon atoms increased in mice treated with PFOA. In brief, the percentages of palmitic acid (C16:0), oleic acid (C18:1), linoleic acid (LA, C18:2), and α-linolenic acid

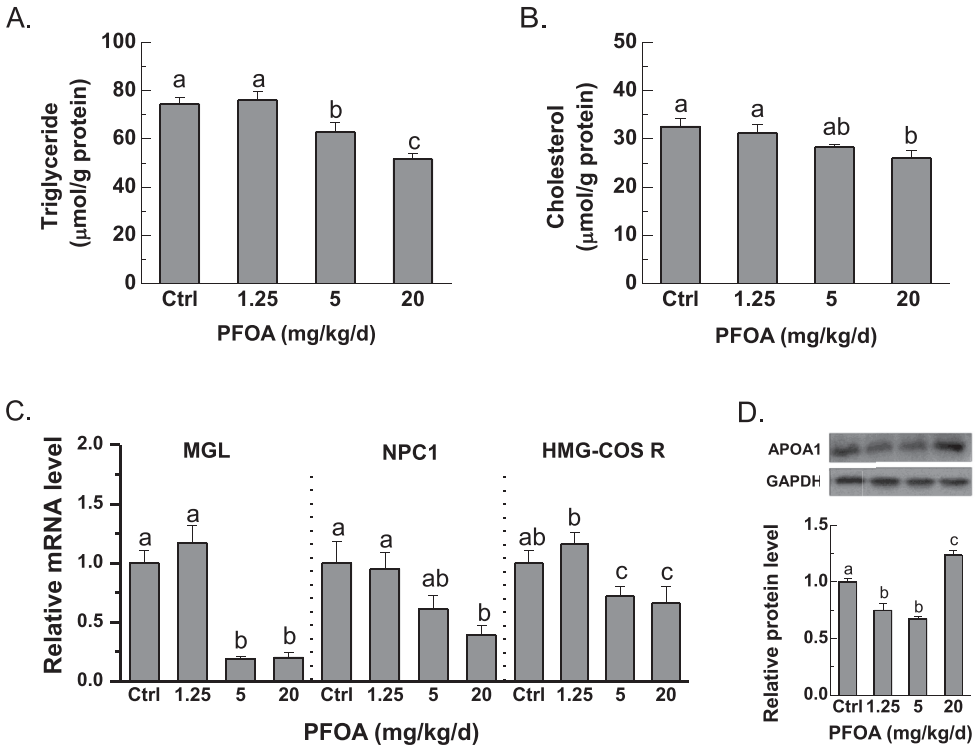

Fig. 2. Levels of lipids and genes in the epididymis. (A) Triglyceride levels in the epididymis, n = 6. (B) Cholesterol levels in the epididymis, n = 6. (C) Triglyceride hydrolysis enzyme MGL mRNA levels, cholesterol metabolism enzyme NPC1 and HMG-COA R mRNA levels, n = 6. (D) Western blot analysis of APOA1 protein levels, n = 3. Mice received either PFOA at 1.25, 5, or 20 mg/kg/d or an equal volume of water for 28 d consecutively. Analyses of A to B were detected by ELISA using epididymis homogenates, C were measured by q-PCR, 18S was set as the internal reference. All data are means ± SE. Values not sharing a common superscript differ significantly at $p < 0.05$ by ANOVA and Duncan's multiple range tests.

(C18:3Δ9,12,5) showed evident decrease, while the percentages of stearic acid (C18:0), arachidonic acid (AA, C20:4Δ5,8,11,14), adrenic acid (C22:4Δ7,10,13,16), docosapentaenoic acid (DPA, C22:5Δ7,10,13,16,19), and docosahexaenoic acid (DHA, C22:6Δ4,7,10,13,16) increased in mice epididymides treated with 5 mg/kg/d PFOA. In addition to the alteration, the AA:LA ratio was significantly increased in mice epididymides treated with 5 mg/kg/d PFOA (Table 1).

3.4. PFOA altered the expression of genes related to PUFA levels

Total RNA of epididymides was extracted from the control and PFOA-treated (1.25, 5, and 20 mg/kg/d) groups. Expression levels of 3-ketoacyl-CoA reductase (KAR, also known as HSD17B12), very long-chain fatty acids, family member 5 (ELOVL5), fatty acid-binding protein 6 (FABP6), and fatty acid-binding protein 7 (FABP7) decreased in the epididymides of the 5 and 20 mg/kg/d PFOA-treated mice (Fig. 2A). Conversely, KAR and fatty acid-binding protein 3 (FABP3) gene levels were increased in the epididymides of the 1.25 mg/kg/d PFOA-treated mice, and FABP4 expression increased in the epididymides in a dose-dependent manner after PFOA exposure (Fig. 3B and C). The expression levels of other related genes, including fatty acid desaturase 1 and 2 (FADS1 and FADS2), *trans*-2,3-enoyl-CoA reductase (TECR), fatty acid-binding protein 1, 2, 5, 9, and 12 (FABP1, FABP2, FABP5, FABP9, and FABP12), and fatty acid transport protein 4 (FATP4, also known as solute carrier family 27 member 4) were not altered (Fig. S2).

3.5. PFOA activated the AKT/AMPK signaling pathway

We examined the fatty acid metabolism-related AKT/AMPK signaling pathway. Epididymis extracts from the control and PFOA-treated (1.25, 5, and 20 mg/kg/d) groups were prepared for western blot analysis. PFOA (5 and 20 mg/kg/d) exposure increased the phosphorylation of AMPK (Thr172) and AKT (Thr308), and subsequently increased the p-AMPK (Thr172)/AMPK and p-AKT (Thr308)/AKT ratios (Fig. 4A–F). The protein expression of AKT and p-AKT (Ser473) and the ratio of p-AKT (Ser473)/AKT were not significantly altered (Fig. 4G–I).

Table 1
Fatty acid composition in the control and 5 mg/kg/d PFOA-treated mice epididymides.

Fatty acid	Mean (±SE) distribution of fatty acid (%)	
	Control	5 mg/kg/d PFOA
Palmitic acid (C16:0)	13.74 ± 0.53	11.41 ± 0.36**
Stearic acid (C18:0)	11.51 ± 1.39	17.74 ± 0.51**
Oleic acid (C18:1Δ^{9})	21.71 ± 0.97	15.65 ± 0.78***
Linoleic acid (C18:2$\Delta^{9,12}$)	20.55 ± 2.23	5.93 ± 1.08***
γ-Linolenic acid (C18:3$\Delta^{6,9,12}$)	0.16 ± 0.00	0.15 ± 0.03
α-Linolenic acid (C18:3$\Delta^{9,12,5}$)	1.17 ± 0.10	0.79 ± 0.04**
Arachidonic acid (C20:4$\Delta^{5,8,11,14}$)	9.53 ± 1.31	17.58 ± 0.62***
EPA (C20:5$\Delta^{5,8,11,14,17}$)	0.39 ± 0.04	0.26 ± 0.03
Adrenic acid (C22:4$\Delta^{7,10,13,16}$)	0.38 ± 0.05	0.77 ± 0.04***
DPA (C22:5$\Delta^{7,10,13,16,19}$)	0.39 ± 0.04	0.57 ± 0.05*
DHA (C22:6$\Delta^{4,7,10,13,16,19}$)	5.16 ± 0.65	7.58 ± 0.26**

Epididymal fatty acids were extracted by chloroform and detected by gas chromatography, n = 6. All data are mean ± SE. *$P < 0.05$, **$P < 0.01$ and ***$P < 0.001$.

3.6. PFOA exposure induced oxidative stress in the epididymis

Epididymis homogenates from the control and PFOA-treated (1.25, 5, and 20 mg/kg/d) groups were prepared in 0.9% NaCl solution for SOD, MDA, and GSH-Px measurement. The levels of MDA

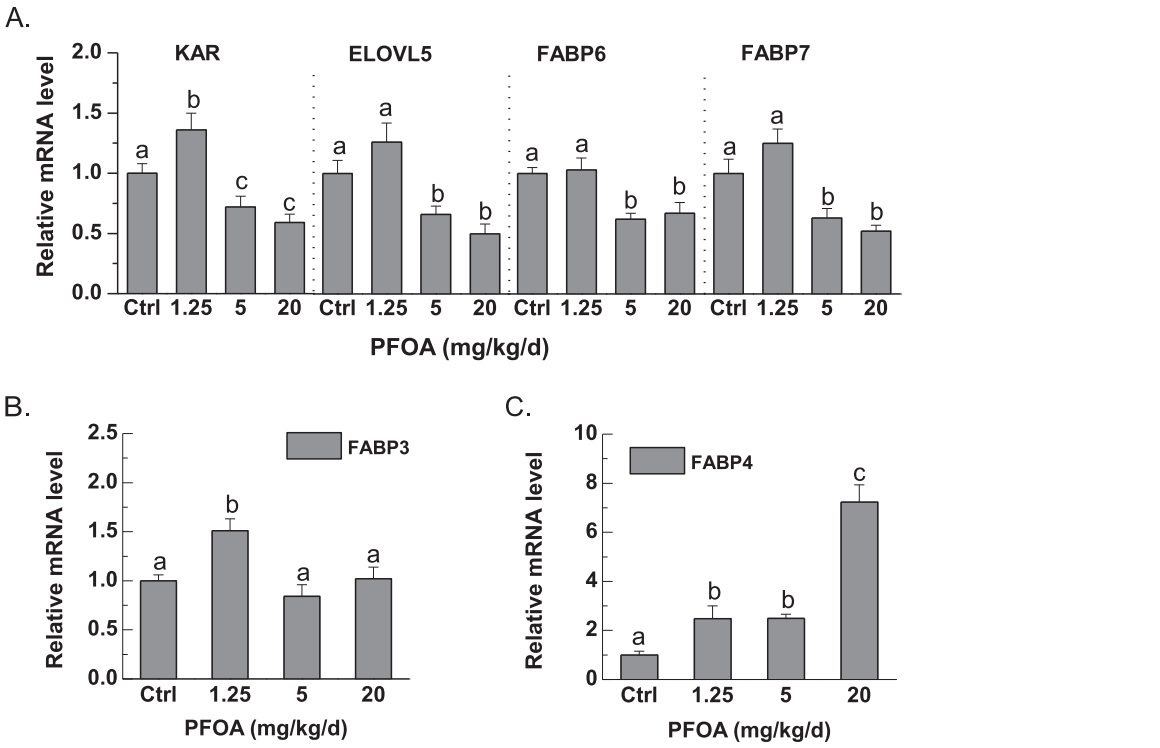

Fig. 3. Levels of genes related to PUFA contents. (A) mRNA levels of PUFA converting enzyme KAR and ELOVL5, FABP6 and FABP7. (B and C) mRNA levels of FABP3 and FABP4. Mice received either PFOA at 1.25, 5, or 20 mg/kg/d or an equal volume of water for 28 d consecutively. Related mRNA levels were measured by q-PCR, 18S was set as the internal reference, n = 6. All data are means ± SE. Values not sharing a common superscript differ significantly at $p < 0.05$ by ANOVA and Duncan's multiple range tests.

were increased in 1.25 and 5 mg/kg/d PFOA exposure groups, and the SOD and MDA ratio was decreased in the 5 mg/kg/d PFOA exposure group (Fig. 5A–C). The levels of GSH-Px were decreased in the 5 and 20 mg/kg/d PFOA exposure groups (Fig. 5D).

3.7. PFOA exposure induced ROS in sperm in vitro

Released sperm were treated with PFOA at doses of 0, 100, or 400 μM, and the ROS levels in sperm were detected at PFOA exposure time points of 1 h, 2 h, 4 h and 8 h. Rosup was used as the positive control as it stimulates ROS release in 20–30 min. In the 100 μM PFOA-treated group, the levels of ROS increased at 1 h and 2 h without altering cell viability, and were not significantly changed at 4 h and 8 h. In the 400 μM PFOA-treated group, the ROS levels increased at every time point, with a slight decrease in cell viability at 8 h (Fig. 6).

4. Discussion

PFOA levels are correlated with reproductive and developmental defects in adults and children (White et al., 2011). In previous study, the level of PFOA in serum following exposure to 0.08 mg/kg/d PFOA in mice was similar to the median serum level of PFOA observed in occupational participants (Wang et al., 2012), and high doses of PFOA have been applied to study sub-acute toxicological effects on male reproduction (Lu et al., 2016). PFOA exposure was shown in our previous study to decrease organ weight, testosterone concentrations, cholesterol content and blood-testis barrier protein expression in the testes in a dose-dependent manner, as well as reduce male mating rates (Lu et al., 2016) and cauda sperm number and motility of mice exposed to 5 mg/kg/d PFOA (Zhang et al., 2014a). In those studies, testicular testosterone synthesis disorder in Leydig cells and blood-testis barrier disturbance between germ cells and Sertoli cells were regarded as possible explanations of male developmental dysfunction caused by PFOA exposure. As an important organ of the male excurrent duct system, the epididymis is a complex sperm migration channel where spermatozoa with progressive motility are stored prior to release through the vas deferens at ejaculation, and is an important organ for achieving sperm fertilizing ability (Belleannee et al., 2012). Here, we studied the effects of PFOA on the epididymis, and showed that PFOA exposure led to high concentrations in the epididymis, as well as reduced epididymis weight and scarce sperm in the epididymal tubules. These results indicate that the epididymis can be affected by PFOA, thus providing another explanation for male developmental dysfunction induced by PFOA exposure. PFOA accumulation and its harmful effects on organ weight have also been reported in male mice livers and testes (Yan et al., 2014; Zhang et al., 2014a). When considering its toxic mechanisms, PFOA is often regarded as a fatty acid disrupting chemical, and exposure can cause lipid imbalance, including CHO, HDL, and TG disorders (Frisbee et al., 2010; Yan et al., 2015). Lipid intracellular levels are balanced between TG synthesis and storage in lipid droplets (Ichimura et al., 2009; Miyauchi et al., 2010). TG and FFA reportedly contribute as important substrates for energy production (Quiroga and Lehner, 2012), and CHO contributes to an impermeable and cohesive membrane in the male reproductive system, modulating male epididymal duct homeostasis to ensure proper post-testicular maturation of male gametes (Saez et al., 2011). In the present study, reduced contents of TG, CHO, and FFA were also observed in the epididymis after PFOA exposure. Similar inhibition effects of PFOA were reported on testis CHO and of PFNA on blood TG and CHO (Zhang et al., 2014a; Wang et al., 2015). Both PFOA and PFNA facilitate TG and CHO accumulation in the liver, in the process of which, hepatic peroxisome proliferator activated receptor alpha (PPARα) and sterol regulatory binding protein

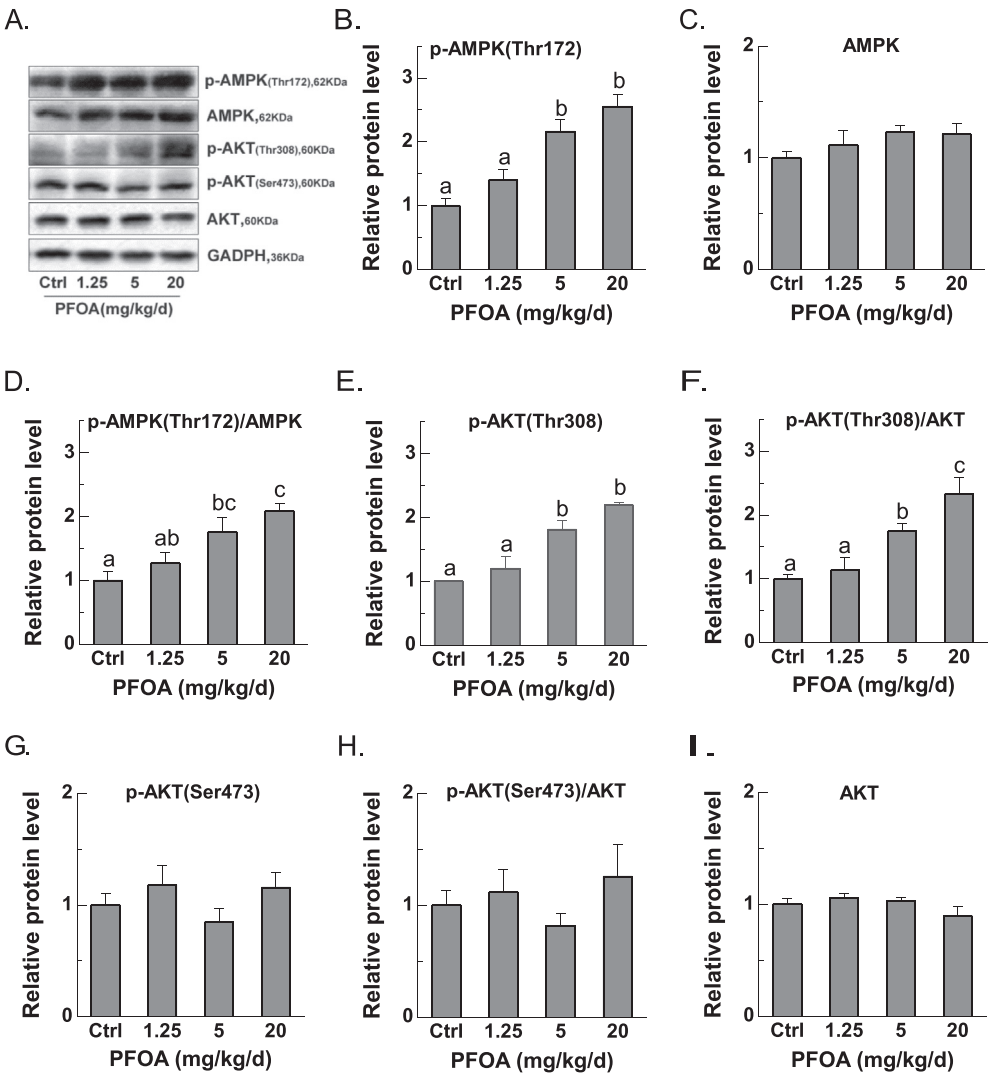

Fig. 4. Protein levels of molecules in AKT/AMPK signaling pathway. (A) Western blot analyses of AKT/AMPK signaling proteins, including p-AMPK (Thr172), AMPK, p-AKT (Thr308), p-AKT (Ser473), and AKT. (B–I) Densitometrically scanned histograms of protein bands. Epididymis lysates (50 μg/well) were loaded onto gels, and reacted with primary and secondary antibodies, GAPDH was set as the loading control and control data were arbitrarily set as 1, n = 3. Values not sharing a common superscript differ significantly at $p < 0.05$ by ANOVA and Duncan's multiple range tests.

(SREBP) activation is crucial (Wang et al., 2015; Yan et al., 2015). In relation to cellular lipid content, monoglyceride lipase (MGL) in most tissues regulates TG lipolysis (Dolinsky et al., 2004; Wendel et al., 2009), HMG-CoA reductase (HMG-COA R), APOA1 (Brundert et al., 2006), and NPC1 (Miller and Bose, 2011), which are responsible for CHO synthesis, uptake, and transfer, respectively. In the present study, the PFOA attenuated gene expressions of MGL, HMG-COA R, and NPC1 supported the decrease in lipid levels in the epididymis. In addition, APOA1 did not exhibit dose-dependency (decreased in the 1.25 and 5 mg/kg/d and increased in the 20 mg/kg/d PFOA group). This might be due to the systematic toxicology of PFOA at high dosage treatment, with similar results reported previously for the liver and testes of mice exposed to 20 mg/kg/d PFOA (Yan et al., 2015; Lu et al., 2016).

PUFAs are important fatty acids, with male rats found to be infertile when raised on a linoleic acid-deficient diet (Leat et al., 1983). In this paper, the significant decrease in linoleic acid might be closely related to male fertility in PFOA-exposed mice. Changes in PUFA composition affects cell membrane fluidity, harms membrane function, and may even lead to death and apoptosis within cells (Labbe et al., 1995; Garcia et al., 2011; Schumann et al., 2011). PUFAs in membranes are prone to lipid peroxidation damage based on the degree of polyunsaturation of the fatty acids, among which DHA is the most susceptible to lipid peroxidation as it has six double bonds (Hulbert et al., 2007). PUFA alteration in the sperm membrane impacts sperm motility and viability, and also the processes that precede and enable the fusion of the spermatozoon with the egg (Yanagimachi, 2012). A reduction in the proportion of PUFA (particularly AA) and an increase in the percentage of saturated fatty acids (particularly palmitic acid) is associated with highly competitive sperm that are morphologically normal, motile, and capable of reaching and fertilizing an egg (Fleming and Yanagimachi, 1984; Waterhouse et al., 2006; delBarco-Trillo et al., 2015). In the present study, increased high unsaturated long chain-PUFA composition concomitant with decreased saturated fatty acid (such as palmitic acid) composition was observed in mice epididymides treated with PFOA. Fatty acid profile disruption has also been found following continuous PFOS and PFOA exposure on freshly fertilized eggs (Arukwe et al., 2013). Cellular PUFA components are associated with enzymes, which convert short chain-

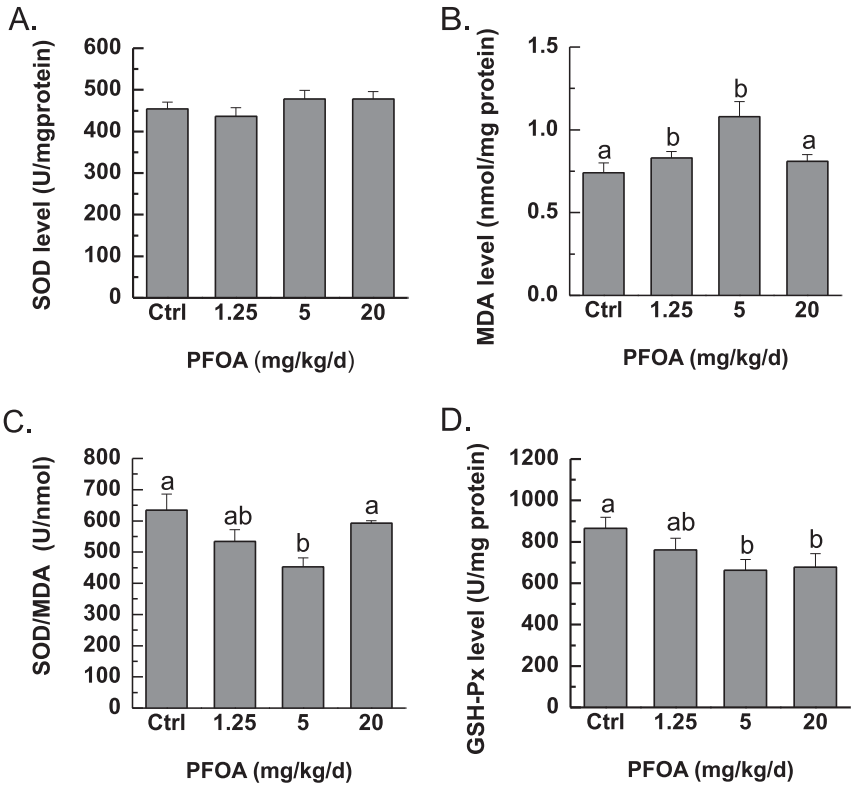

Fig. 5. Oxidative index after PFOA treatment in the epididymis. (A) Level of SOD in the epididymis. (B) Level of MDA in the epididymis. (C) Ratio of SOD/MDA in the epididymis. (D) Level of GSH-Px in the epididymis. Epididymides from the control and PFOA exposure groups (1.25, 5, and 20 mg/kg/d) were obtained and homogenates prepared. Oxidative indexes were normalized to epididymal protein concentration. All data are means ± SE, n = 6. Values not sharing a common superscript differ significantly at $p < 0.05$ by ANOVA and Duncan's multiple range tests.

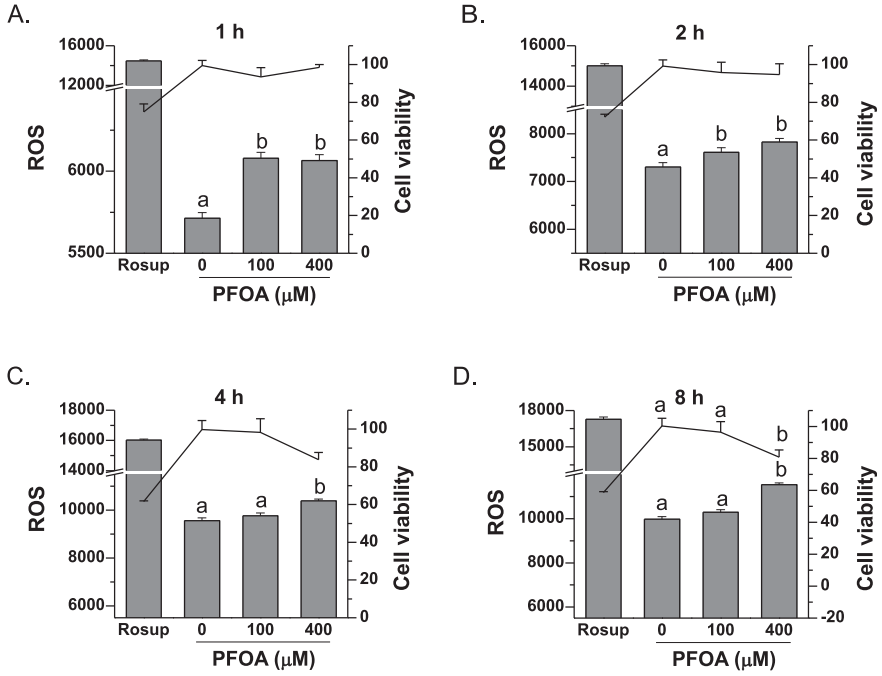

Fig. 6. Time dependent sperm ROS release induced by PFOA *in vitro*. Sperm were released from healthy adult BABL/c mice, and loaded with DCFH-DA, a ROS probe, followed by PFOA treatment at doses of 0, 100, or 400 μM. Treatment was terminated at 1 h, 2 h, 4 h and 8 h, and DCF fluorescence and relative cell viability were detected per well. (A–D) Cell viability and ROS levels at four time points, all ROS levels were normalized to cell viability. All data are means ± SE, n = 6. Values not sharing a common superscript differ significantly at $p < 0.05$ by ANOVA and Duncan's multiple range tests.

PUFAs into long chain-PUFAs under pathological conditions, even though the conversion rate is very low in physiological status. Correspondingly, enzyme expressions are stimulated by fatty acid-deficiencies (Saether et al., 2007). KAR and ElOVL5 are two elongation enzymes that covert precursors to stearic acid and γ-linolenic acid, respectively (Berquin et al., 2011). In this paper, those two genes showed attenuation consistent with abundant stearic and γ-linolenic acid in mice treated with 5 mg/kg/d PFOA. FABPs, uptake fatty acid in mammalian tissue, are also associated with PUFA content. FABPs exhibit high binding affinity to single saturated or unsaturated long-chain fatty acid (≥14 carbons) molecules, accelerating FUFA uptake and intracellular transport into remote peripheral tissues (Ono, 2005), and FABPs contents are mostly regulated at the transcriptional level (Storch and Thumser, 2010). In our research, the downregulated expression of KAR, ELOVL5 and FABPs genes provided evidence for the saturated PUFA decrease in the mice epididymides, except for FABP4 which showed a dose-response increase after PFOA exposure. Increase in the transcriptional level of FABP4 might be a compensatory effect due to PFOA accumulation in organ, as PFOA displays a moderate affinity for FABP4 at a 1:1 M ratio (Sheng et al., 2016). Recognized as an energy sensor, AMPK plays an important role in energy homeostasis and nutrient metabolism by reversible phosphorylation activation at the Thr172 site (O'Neill et al., 2013). Once activated, AMPK initiates fatty acid oxidation, also maintaining cellular energy homeostasis by turning on catabolic pathways that generate ATP and switching off nonessential ATP-consuming processes (Hardie et al., 2012). Studies have indicated that AMPK and its downstream signaling pathway are involved in fat consumption in both cell lines and laboratory animals (Gong et al., 2015; Lee et al., 2015). Here, increased AMPK phosphorylation at the Thr172 site was observed, indicating the occurrence of AMPK activation in the epididymides of PFOA-exposed mice. Akt is activated by phospholipid binding and activation loop phosphorylation at the Thr308 site by PDK1 (Franke et al., 1995) and by phosphorylation within the carboxy terminus at the Ser473 site by PDK2 (Cross et al., 1995). Deletion of the AKT gene markedly decreases intracellular ATP levels in knockout mouse embryonic fibroblasts (Gottlob et al., 2001). In the present study, increased AKT phosphorylation at Thr308, indicating AKT activation, was also observed in mice epididymides after PFOA treatment. These results implied disturbance of substances associated with cellular energy production, such as TG stores and CHO contents in the epididymis. In addition, the phosphorylation of AMPK at the conserved Thr172 residue can be inactivated by two enzymes involved in lipid synthesis, i.e., acetyl-CoA carboxylase and HMG-COA R in the α2-subunit (Carlson and Kim, 1974; Carling et al., 1987). AA has been reported to function in the activation of the AMPK protein through phosphorylation at the Thr172 residue in primary rat hepatocytes (Kohan et al., 2009). In the present study, the decrease in the HMG-COA R expression levels and increase in AA levels were conducive to AMPK activation by phosphorylation at the Thr172 residue. AA also contributes to oxidative stress during phospholipid oxidation, and AA can cause cells to produce excess ROS in the presence of iron (Shin and Kim, 2009). Excess ROS modifies the phospholipids of fatty acid within the cell membrane (Valko et al., 2006). During this process, AA is further released from the cellular membrane lipid bilayer, enhancing oxidative stress during phospholipid oxidation (Balboa and Balsinde, 2006). Cascading ROS can damage cells and tissues through the deleterious modification of membrane phospholipids, causing oxidative stress and inducing mitochondrial dysfunction and apoptosis or even cell death (Stark, 2005). Here, decreased LA and increased AA levels, concomitant with promoted oxidative stress, such as a decrease in GSH-Px and increase in oxidation product MDA, were observed in mice epididymides treated with 5 mg/kg/d PFOA, indicating that oxidative stress occurred in the epididymis and the antioxidant defense system failed to resist oxidative substances. Moreover, mitochondria are rich in acrosome because a constant supply of energy is required for sperm motility, but the main source of ROS is also from the mitochondria (Chen et al., 2013). However, sperm are equipped with antioxidant defense mechanisms and are likely to quench ROS, thereby protecting mature spermatozoa from oxidative damage. When the production of ROS exceeds the antioxidant capacity of the seminal plasma, oxidative stress will still result (Henkel, 2011). While small amounts of ROS are required for normal sperm function, under pathological conditions, augmented ROS production can negatively impact the quality of spermatozoa and impair their overall fertilizing capacity (Trussell, 2013). In the present study, time dependent production of ROS was also induced in released sperm treated with 400 μM of PFOA *in vitro*, indicating that PFOA can induce excessive ROS production in sperm. In addition, AMPK can be activated by an altered AMP:ATP ratio under stress, and also activated directly or indirectly by increased levels of cytoplasmic ROS to protect the cell against oxidative stress (Jager et al., 2007).

5. Conclusions

PFOA is a potent reproductive toxin, which can deleteriously affect the epididymis in male mice. In the current research, PFOA exposure caused epididymis weight loss, TG, CHO and FFA content decrease, and AKT/AMPK signaling pathway activation in the epididymis. Alteration in PUFA composition, especially increased unsaturated long chain-PUFAs, might be an important reason for PFOA-induced male reproductive dysfunction. Moreover, the disturbance of PUFAs likely induced oxidative stress in the epididymis, and might also go part way to explaining male reproductive dysfunction. However, further study is needed to investigate the role of ROS in those processes.

Acknowledgments

This work was supported by the Natural Science Foundation of China (Grant: 31320103915) and the National Basic Research Program of China (973; Grant: 2013CB945204).

Appendix A. Supplementary data

Supplementary data related to this article can be found at http://dx.doi.org/10.1016/j.chemosphere.2016.05.071.

References

Arukwe, A., Cangialosi, M.V., Letcher, R.J., Rocha, E., Mortensen, A.S., 2013. Changes in morphometry and association between whole-body fatty acids and steroid hormone profiles in relation to bioaccumulation patterns in salmon larvae exposed to perfluorooctane sulfonic or perfluorooctane carboxylic acids. Aquat. Toxicol. 130–131, 219–230.

Auten, R.L., Davis, J.M., 2009. Oxygen toxicity and reactive oxygen species: the devil is in the details. Pediatr. Res. 66, 121–127.

Balboa, M.A., Balsinde, J., 2006. Oxidative stress and arachidonic acid mobilization. Biochim. Biophys. Acta 1761, 385–391.

Bellacosa, A., Testa, J.R., Staal, S.P., Tsichlis, P.N., 1991. A retroviral oncogene, akt, encoding a serine-threonine kinase containing an SH2-like region. Science 254, 274–277.

Belleannee, C., Thimon, V., Sullivan, R., 2012. Region-specific gene expression in the epididymis. Cell Tissue Res. 349, 717–731.

Berquin, I.M., Edwards, I.J., Kridel, S.J., Chen, Y.Q., 2011. Polyunsaturated fatty acid metabolism in prostate cancer. Cancer metastasis Rev. 30, 295–309.

Brundert, M., Heeren, J., Bahar-Bayansar, M., Ewert, A., Moore, K.J., Rinninger, F., 2006. Selective uptake of HDL cholesteryl esters and cholesterol efflux from mouse peritoneal macrophages independent of SR-BI. J. lipid Res. 47, 2408–2421.

Carling, D., Zammit, V.A., Hardie, D.G., 1987. A common bicyclic protein kinase cascade inactivates the regulatory enzymes of fatty acid and cholesterol

biosynthesis. FEBS Lett. 223, 217–222.
Carlson, C.A., Kim, K.H., 1974. Regulation of hepatic acetyl coenzyme A carboxylase by phosphorylation and dephosphorylation. Arch. Biochem. Biophys. 164, 478–489.
Chen, S.J., Allam, J.P., Duan, Y.G., Haidl, G., 2013. Influence of reactive oxygen species on human sperm functions and fertilizing capacity including therapeutical approaches. Arch. Gynecol. Obstet. 288, 191–199.
Cross, D.A., Alessi, D.R., Cohen, P., Andjelkovich, M., Hemmings, B.A., 1995. Inhibition of glycogen synthase kinase-3 by insulin mediated by protein kinase B. Nature 378, 785–789.
delBarco-Trillo, J., Mateo, R., Roldan, E.R., 2015. Differences in the fatty-acid composition of rodent spermatozoa are associated to levels of sperm competition. Biol. Open 4, 466–473.
Dimitrov, S., Kamenska, V., Walker, J.D., Windle, W., Purdy, R., Lewis, M., Mekenyan, O., 2004. Predicting the biodegradation products of perfluorinated chemicals using CATABOL. SAR QSAR Environ. Res. 15, 69–82.
Dolinsky, V.W., Douglas, D.N., Lehner, R., Vance, D.E., 2004. Regulation of the enzymes of hepatic microsomal triacylglycerol lipolysis and re-esterification by the glucocorticoid dexamethasone. Biochem. J. 378, 967–974.
Dong, G.Z., Jang, E.J., Kang, S.H., Cho, I.J., Park, S.D., Kim, S.C., Kim, Y.W., 2013. Red ginseng abrogates oxidative stress via mitochondria protection mediated by LKB1-AMPK pathway. BMC Complementary Altern. Med. 13, 64.
Feng, Y., Fang, X., Shi, Z., Xu, M., Dai, J., 2010. Effects of PFNA exposure on expression of junction-associated molecules and secretory function in rat Sertoli cells. Reprod. Toxicol. 30, 429–437.
Feng, Y., Shi, Z., Fang, X., Xu, M., Dai, J., 2009. Perfluorononanoic acid induces apoptosis involving the Fas death receptor signaling pathway in rat testis. Toxicol. Lett. 190, 224–230.
Fleming, A.D., Yanagimachi, R., 1984. Evidence suggesting the importance of fatty acids and the fatty acid moieties of sperm membrane phospholipids in the acrosome reaction of guinea pig spermatozoa. J. Exp. Zool. 229, 485–489.
Franke, T.F., Yang, S.I., Chan, T.O., Datta, K., Kazlauskas, A., Morrison, D.K., Kaplan, D.R., Tsichlis, P.N., 1995. The protein kinase encoded by the Akt proto-oncogene is a target of the PDGF-activated phosphatidylinositol 3-kinase. Cell 81, 727–736.
Frisbee, S.J., Shankar, A., Knox, S.S., Steenland, K., Savitz, D.A., Fletcher, T., Ducatman, A.M., 2010. Perfluorooctanoic acid, perfluorooctanesulfonate, and serum lipids in children and adolescents: results from the C8 Health Project. Arch. Pediatr. Adolesc. Med. 164, 860–869.
Funari, S.S., Barcelo, F., Escriba, P.V., 2003. Effects of oleic acid and its congeners, elaidic and stearic acids, on the structural properties of phosphatidylethanolamine membranes. J. lipid Res. 44, 567–575.
Garcia, B.M., Fernandez, L.G., Ferrusola, C.O., Salazar-Sandoval, C., Rodriguez, A.M., Martinez, H.R., Tapia, J.A., Morcuende, D., Pena, F.J., 2011. Membrane lipids of the stallion spermatozoon in relation to sperm quality and susceptibility to lipid peroxidation. Reprod. Domest. Anim.Zuchthyg. 46, 141–148.
Gong, M., Cao, C., Chen, F., Li, Q., Bi, X., Sun, Y., Zhan, Z., 2015. Electroacupuncture attenuates hepatic lipid accumulation via AMP-activated protein kinase (AMPK) activation in obese rats. Acupunct. Med. J. Br. Med. Acupunct. Soc. http://dx.doi.org/10.1136/acupmed-2015-010798 [Epub ahead of print].
Gottlob, K., Majewski, N., Kennedy, S., Kandel, E., Robey, R.B., Hay, N., 2001. Inhibition of early apoptotic events by Akt/PKB is dependent on the first committed step of glycolysis and mitochondrial hexokinase. Genes & Dev. 15, 1406–1418.
Hansen, K.J., Clemen, L.A., Ellefson, M.E., Johnson, H.O., 2001. Compound-specific, quantitative characterization of organic fluorochemicals in biological matrices. Environ. Sci. Technol. 35, 766–770.
Hardie, D.G., Ross, F.A., Hawley, S.A., 2012. AMPK: a nutrient and energy sensor that maintains energy homeostasis. Nat. Rev. Mol. Cell Biol. 13, 251–262.
Henkel, R.R., 2011. Leukocytes and oxidative stress: dilemma for sperm function and male fertility. Asian J. Androl. 13, 43–52.
Hulbert, A.J., Pamplona, R., Buffenstein, R., Buttemer, W.A., 2007. Life and death: metabolic rate, membrane composition, and life span of animals. Physiol. Rev. 87, 1175–1213.
Ichimura, A., Hirasawa, A., Hara, T., Tsujimoto, G., 2009. Free fatty acid receptors act as nutrient sensors to regulate energy homeostasis. Prostagl. Other Lipid Mediat. 89, 82–88.
Jager, S., Handschin, C., St-Pierre, J., Spiegelman, B.M., 2007. AMP-activated protein kinase (AMPK) action in skeletal muscle via direct phosphorylation of PGC-1alpha. Proc. Natl. Acad. Sci. U. S. A. 104, 12017–12022.
Kohan, A.B., Talukdar, I., Walsh, C.M., Salati, L.M., 2009. A role for AMPK in the inhibition of glucose-6-phosphate dehydrogenase by polyunsaturated fatty acids. Biochem. Biophys. Res. Commun. 388, 117–121.
Labbe, C., Maisse, G., Muller, K., Zachowski, A., Kaushik, S., Loir, M., 1995. Thermal acclimation and dietary lipids alter the composition, but not fluidity, of trout sperm plasma membrane. Lipids 30, 23–33.
Lan, A., Du, J., 2015. Potential role of Akt signaling in chronic kidney disease. Nephrology, dialysis, transplantation. Off. Publ. Eur. Dial. Transpl. Assoc. Eur. Ren. Assoc. 30, 385–394.
Leat, W.M., Northrop, C.A., Harrison, F.A., Cox, R.W., 1983. Effect of dietary linoleic and linolenic acids on testicular development in the rat. Q. J. Exp. Physiol. 68, 221–231.
Lee, J.H., Kim, T., Lee, J.J., Lee, K.J., Kim, H.K., Yun, B., Jeon, J., Kim, S.K., Ma, J.Y., 2015. The herbal medicine KBH-1 inhibits fat accumulation in 3T3-L1 adipocytes and reduces high fat diet-induced obesity through regulation of the AMPK pathway. PLoS One 10, e0142041.
Lehmler, H.J., 2005. Synthesis of environmentally relevant fluorinated surfactants–a review. Chemosphere 58, 1471–1496.
Liu, L., Liu, Y., Cui, J., Liu, H., Liu, Y.B., Qiao, W.L., Sun, H., Yan, C.D., 2013. Oxidative stress induces gastric submucosal arteriolar dysfunction in the elderly. World J. Gastroenterol. 19, 9439–9446.
Loh, K.P., Qi, J., Tan, B.K., Liu, X.H., Wei, B.G., Zhu, Y.Z., 2010. Leonurine protects middle cerebral artery occluded rats through antioxidant effect and regulation of mitochondrial function. Stroke 41, 2661–2668.
Lu, Y., Luo, B., Li, J., Dai, J., 2016. Perfluorooctanoic acid disrupts the blood-testis barrier and activates the TNFalpha/p38 MAPK signaling pathway in vivo and in vitro. Arch. Toxicol. 90, 971–983.
Mantzaris, M.D., Tsianos, E.V., Galaris, D., 2011. Interruption of triacylglycerol synthesis in the endoplasmic reticulum is the initiating event for saturated fatty acid-induced lipotoxicity in liver cells. FEBS J. 278, 519–530.
Miller, W.L., Bose, H.S., 2011. Early steps in steroidogenesis: intracellular cholesterol trafficking. J. Lipid Res. 52, 2111–2135.
Miyauchi, S., Hirasawa, A., Ichimura, A., Hara, T., Tsujimoto, G., 2010. New frontiers in gut nutrient sensor research: free fatty acid sensing in the gastrointestinal tract. J. Pharmacol. Sci. 112, 19–24.
O'Neill, H.M., Holloway, G.P., Steinberg, G.R., 2013. AMPK regulation of fatty acid metabolism and mitochondrial biogenesis: implications for obesity. Mol. Cell. Endocrinol. 366, 135–151.
Ono, T., 2005. Studies of the FABP family: a retrospective. Mol. Cell. Biochem. 277, 1–6.
Papackova, Z., Cahova, M., 2015. Fatty acid signaling: the new function of intracellular lipases. Int. J. Mol. Sci. 16, 3831–3855.
Pico, Y., Farre, M., Llorca, M., Barcelo, D., 2011. Perfluorinated compounds in food: a global perspective. Crit. Rev. Food Sci. Nutr. 51, 605–625.
Prevedouros, K., Cousins, I.T., Buck, R.C., Korzeniowski, S.H., 2006. Sources, fate and transport of perfluorocarboxylates. Environ. Sci. Technol. 40, 32–44.
Quiroga, A.D., Lehner, R., 2012. Liver triacylglycerol lipases. Biochim. Biophys. Acta 1821, 762–769.
Saether, T., Tran, T.N., Rootwelt, H., Grav, H.J., Christophersen, B.O., Haugen, T.B., 2007. Essential fatty acid deficiency induces fatty acid desaturase expression in rat epididymis, but not in testis. Reproduction 133, 467–477.
Saez, F., Ouvrier, A., Drevet, J.R., 2011. Epididymis cholesterol homeostasis and sperm fertilizing ability. Asian J. Androl. 13, 11–17.
Samovski, D., Sun, J., Pietka, T., Gross, R.W., Eckel, R.H., Su, X., Stahl, P.D., Abumrad, N.A., 2015. Regulation of AMPK activation by CD36 links fatty acid uptake to beta-oxidation. Diabetes 64, 353–359.
Schumann, J., Leichtle, A., Thiery, J., Fuhrmann, H., 2011. Fatty acid and peptide profiles in plasma membrane and membrane rafts of PUFA supplemented RAW264.7 macrophages. PLoS One 6, e24066.
Sheng, N., Li, J., Liu, H., Zhang, A., Dai, J., 2016. Interaction of perfluoroalkyl acids with human liver fatty acid-binding protein. Arch. Toxicol. 90, 217–227.
Shin, S.M., Cho, I.J., Kim, S.G., 2009. Resveratrol protects mitochondria against oxidative stress through AMP-activated protein kinase-mediated glycogen synthase kinase-3beta inhibition downstream of poly(ADP-ribose)polymerase-LKB1 pathway. Mol. Pharmacol. 76, 884–895.
Shin, S.M., Kim, S.G., 2009. Inhibition of arachidonic acid and iron-induced mitochondrial dysfunction and apoptosis by oltipraz and novel 1,2-dithiole-3-thione congeners. Mol. Pharmacol. 75, 242–253.
Stark, G., 2005. Functional consequences of oxidative membrane damage. J. Membr. Biol. 205, 1–16.
Steenland, K., Tinker, S., Frisbee, S., Ducatman, A., Vaccarino, V., 2009. Association of perfluorooctanoic acid and perfluorooctane sulfonate with serum lipids among adults living near a chemical plant. Am. J. Epidemiol. 170, 1268–1278.
Storch, J., Thumser, A.E., 2010. Tissue-specific functions in the fatty acid-binding protein family. J. Biol. Chem. 285, 32679–32683.
Thomas, A., Pepper, C., Hoy, T., Bentley, P., 2004. Bryostatin induces protein kinase C modulation, Mcl-1 up-regulation and phosphorylation of Bcl-2 resulting in cellular differentiation and resistance to drug-induced apoptosis in B-cell chronic lymphocytic leukemia cells. Leuk. Lymphoma 45, 997–1008.
Trussell, J.C., 2013. Optimal diagnosis and medical treatment of male infertility. Semin. Reprod. Med. 31, 235–236.
Valko, M., Rhodes, C.J., Moncol, J., Izakovic, M., Mazur, M., 2006. Free radicals, metals and antioxidants in oxidative stress-induced cancer. Chem. Biol. Interact. 160, 1–40.
Wang, J., Yan, S., Zhang, W., Zhang, H., Dai, J., 2015. Integrated proteomic and miRNA transcriptional analysis reveals the hepatotoxicity mechanism of PFNA exposure in mice. J. Proteom. Res. 14, 330–341.
Wang, J., Zhang, Y., Zhang, W., Jin, Y., Dai, J., 2012. Association of perfluorooctanoic acid with HDL cholesterol and circulating miR-26b and miR-199-3p in workers of a fluorochemical plant and nearby residents. Environ. Sci. Technol. 46, 9274–9281.
Wang, N., Szostek, B., Buck, R.C., Folsom, P.W., Sulecki, L.M., Gannon, J.T., 2009. 8-2 fluorotelomer alcohol aerobic soil biodegradation: pathways, metabolites, and metabolite yields. Chemosphere 75, 1089–1096.
Waterhouse, K.E., Hofmo, P.O., Tverdal, A., Miller Jr., R.R., 2006. Within and between breed differences in freezing tolerance and plasma membrane fatty acid composition of boar sperm. Reproduction 131, 887–894.
Wendel, A.A., Lewin, T.M., Coleman, R.A., 2009. Glycerol-3-phosphate acyltransferases: rate limiting enzymes of triacylglycerol biosynthesis. Biochim. Biophys. Acta 1791, 501–506.
White, S.S., Fenton, S.E., Hines, E.P., 2011. Endocrine disrupting properties of

perfluorooctanoic acid. J. Steroid Biochem. Mol. Biol. 127, 16–26.
Yan, S., Wang, J., Dai, J., 2015. Activation of sterol regulatory element-binding proteins in mice exposed to perfluorooctanoic acid for 28 days. Arch. Toxicol. 89, 1569–1578.
Yan, S., Wang, J., Zhang, W., Dai, J., 2014. Circulating microRNA profiles altered in mice after 28 d exposure to perfluorooctanoic acid. Toxicol. Lett. 224, 24–31.
Yanagimachi, R., 2012. Fertilization studies and assisted fertilization in mammals: their development and future. J. Reprod. Dev. 58, 25–32.
Zeng, H.L., Huang, S.L., Xie, F.C., Zeng, L.M., Hu, Y.H., Leng, Y., 2015. Yhhu981, a novel compound, stimulates fatty acid oxidation via the activation of AMPK and ameliorates lipid metabolism disorder in ob/ob mice. Acta Pharmacol. Sin. 36, 343–352.
Zhang, H., Lu, Y., Luo, B., Yan, S., Guo, X., Dai, J., 2014a. Proteomic analysis of mouse testis reveals perfluorooctanoic acid-induced reproductive dysfunction via direct disturbance of testicular steroidogenic machinery. J. Proteom. Res. 13, 3370–3385.
Zhang, M., Feng, L., Gu, J., Ma, L., Qin, D., Wu, C., Jia, X., 2014b. The attenuation of Moutan Cortex on oxidative stress for renal injury in AGEs-induced mesangial cell dysfunction and streptozotocin-induced diabetic nephropathy rats. Oxid. Med. Cell. Longev. 2014, 463815.